3-Bromohomofascaplysin A, a fascaplysin analogue from a Fijian *Didemnum* sp. ascidian

Zhenyu Lu[a], **Yuanqing Ding**[b], **Xing-Cong Li**[b], **Daignon R. Djigbenou**[c,d], **Brian T. Grimberg**[d], **Daneel Ferreira**[b], **Chris M. Ireland**[a], and **Ryan M. Van Wagoner**[a,*]

[a] Department of Medicinal Chemistry, University of Utah, Salt Lake City, UT 84112, USA

[b] Department of Pharmacognosy and National Center for Natural Products Research, School of Pharmacy, University of Mississippi, University, MS 38677, USA

[c] Division of Infectious Disease, Case Western Reserve University, Cleveland, OH 44106, USA

[d] Center for Global Health & Diseases, Case Western Reserve University, Cleveland, OH 44106, USA

Abstract

A new fascaplysin analogue, 3-bromohomofascaplysin A (**1**), along with two known analogues, homofascaplysin A (**2**) and fascaplysin (**3**), were isolated from a Fijian *Didemnum* sp. ascidian. The absolute configurations of 3-bromohomofascaplysin A (**1**) and homofascaplysin A (**2**) were determined via experimental and theoretically calculated ECD spectra. The differential activities of **1**–**3** against different blood-borne life stages of the malaria pathogen *Plasmodium falciparum* were assessed. Homofascaplysin A (**2**) displayed an IC_{50} of 0.55 ± 0.11 nM against ring stage parasites and 105 ± 38 nM against all live parasites. Given the stronger resistance of ring stage parasites against most current antimalarials relative to the other blood stages, homofascaplysin A (**2**) represents a promising agent for treatment of drug resistant malaria.

Keywords

Fascaplysin analogues; ascidian; antimalarial; absolute configuration; experimental and theoretically calculated ECD

1. Introduction

Fascaplysin (**3**), originally isolated from a marine sponge *Fascaplysinopsis* sp.,[1] displays a variety of biological activities, such as selective CDK 4 inhibition,[2,3] DNA binding,[4] and both *in vitro* and *in vivo* anti-angiogenic effects.[5] We revisited the ascidian, *Didemnum* sp., that we previously studied[6] and discovered a new related compound, 3-bromohomofascaplysin A (**1**), along with homofascaplysin A (**2**)[7,8] and fascaplysin (**3**).[1] The genus *Didemnum* is known to contain structurally diverse biologically active compounds such as cyclic peptides with characteristic modified amino acids,[9]

Publisher's Disclaimer: This is a PDF file of an unedited manuscript that has been accepted for publication. As a service to our customers we are providing this early version of the manuscript. The manuscript will undergo copyediting, typesetting, and review of the resulting proof before it is published in its final citable form. Please note that during the production process errors may be discovered which could affect the content, and all legal disclaimers that apply to the journal pertain.

pyridoacridines,[10] β-carbolines,[11] lamellarin,[12] 3,4-substituted maleimides,[13] and polysulfide alkaloids.[14] Herein we report the isolation and structure elucidation of the new compound **1**, the determination of the absolute configuration of **1** and **2** by electronic circular dichroism (ECD) methods, and the differential activities of **1**–**3** against blood-borne life stages of the malaria pathogen *Plasmodium falciparum*.

2. Results and Discussion

Compound **1** was isolated as an amorphous pale yellow-brown solid. The positive ESIMS of **1** showed a molecular ion cluster at *m/z* 407/409 (1:1) M[+] diagnostic for a monobrominated molecule. The molecular formula was determined as $C_{21}H_{16}N_2O_2Br$ by HRESIMS. The ^1H NMR spectrum (Table 1) displayed one methyl at δ_H 1.99, one methylene at δ_H 4.26/4.16 and nine aromatic protons at δ_H 9.26, 8.77, 8.54, 8.43, 7.80, 7.82 (2H), 7.83, and 7.49. The ^{13}C NMR spectrum (Table 1) revealed 21 carbons including one carbonyl carbon, 17 aromatic carbons, one oxygenated quaternary carbon, one methylene, and one methyl carbon.

The ^1H NMR data were similar to those reported for homofascaplysin A (**2**),[7] the major difference being the loss of an aromatic proton signal in **1** compared to **2**. Comparison of the molecular formulae of **1** and **2** showed that **1** was the bromo-analogue of **2**. Inspection of the ^1H NMR spectrum of **1** revealed the presence of one *meta*-coupled aromatic proton (δ_H 8.54, *J* = 1.2 Hz), indicating the Br was positioned at either C-2, C-3, C-9 or C-10. Comparison of the ^{13}C NMR data of **1** with **2** indicated significant shifts of the E-ring carbons, suggesting attachment of the Br atom at C-2 or C-3. The ROESY experiment showed a correlation between H-6 and the *meta*-coupled proton allowing assignment of this signal to H-4 and hence attachment of the Br atom at C-3. HMBC data provided unambiguous evidence confirming the structural assignment.

The identity of the known compounds homofascaplysin A (**2**) and fascaplysin (**3**) were readily confirmed by comparison of their spectroscopic properties with literature data.[1,7,8]

The absolute configuration of **2** was assigned by comparison of the experimental ECD spectrum with simulated spectra calculated by time-dependent density functional theory (TDDFT).[15] The model was arbitrarily assigned a configuration of 13*S*. The potential energy surface was scanned in the gas phase at the AM1 level by rotating about the C-14-C-13 and C-15-C-14 bonds (Figure S-1). Of the six conformers that were located, only three (**2a**-**2c**) were relocated at the B3LYP/6-31G** level in the gas phase with conformational distributions of 20.5%, 0.4% and 79.1%, respectively, as calculated from electronic and zero-point energies (Figure S-2 and Table S-1). The distributions for **2a**–**2c** shifted to 41.8%, 2.2% and 56.0%, respectively, at the B3LYP-SCRF/6-31G**//B3LYP/6-31G** level in MeOH with COSMO model, indicating that solvent effects are significant for this cationic system. The prominent differences between the optimized geometries are the presence of (C-15)O···H-O(C-13) hydrogen bonding in **2a** and both (C-15)O···H-O(C-13) and (C15)O···H-N-12 hydrogen bonding in **2c** (Figure S-2 and Table S-3). ECD spectra of individual conformers have been calculated at the B3LYP/6-31G** level in the gas phase and at the B3LYP-SCRF/6-31G**//B3LYP/6-31G** level in MeOH with the COSMO model (Figure S-3). The weighted average ECD spectra of conformers **2a**–**2c** in both the gas phase and MeOH are depicted in Figure 1 alongside the experimental ECD spectrum for **2**. Experimentally observed negative Cotton effects at 334 and 275 nm correlate well with predicted electronic transitions at 345 and 272 nm for conformer **2a** and at 345 nm and 262 nm for conformer **2c**, respectively, calculated in MeOH at the B3LYP-SCRF/6-31G**// B3LYP/6-31G** level (Figure S-3). Thus, an absolute configuration of 13*S* was unambiguously determined for **2**. The absolute configuration of **1** was also assigned as 13*S*

based on the similarity of its CD spectrum to that of **2** (Figure 2). Such assignment was additionally supported by the similar specific rotations of compounds **1** and **2** (−9.0° and −9.38°,[7] respectively).

A previous study had shown that homofascaplysin A (**2**) and fascaplysin (**3**) each exhibited activity with IC_{50} values of 38 nM and 160 nM,[8] respectively, against the chloroquine- and pyrimethamine-resistant *Plasmodium falciparum* strain K1. In order to further probe the potential for use of fascaplysins against resistant *P. falciparum*, the blood-borne life stage-specific activities[16] of compounds **1**–**3** against the highly resistant strain W2-Mef were determined. The results are shown in Table 2. Compounds **1** and **2** displayed overall IC_{50} values comparable to the previously reported values against the strain K1.[16] Moreover, each of **1**–**3** exhibited greater potency against the ring stage parasites compared to the trophozoite and schizont stages. Of the three compounds, **1** was the least potent and **3** the most potent overall. However, **2** exhibited the strongest selectivity for ring stage parasites with a stage-specific IC_{50} value of 0.55 nM, representing a 450-fold and 170-fold selectivity for ring stage over trophozoite and schizont stages, respectively. Since ring-stage parasites are typically two-fold less sensitive to many first line antimalarials such as chloroquine,[16] the fascaplysins and particularly **2** represent promising lead compounds for the treatment of resistant malaria.

The fascaplysins bear strong structural similarities to the cryptolepines, another indole-containing family of antimalarial compounds.[17] Like fascaplysin, cryptolepine has DNA intercalating activity.[18] Cryptolepine has additionally been shown to inhibit formation of hemozoin in *P. falciparum*,[17] though synthetic studies with other cryptolepine analogues have suggested that other mechanisms are responsible for their activity.[19] It is interesting to note that bromination of cryptolepines generally increased potency[19] whereas for the fascaplysins, **1** is considerably less potent than **2**. In the earlier study describing antimalarial activities for **2** and **3**,[8] cytotoxicity against skeletal rat muscle myoblast cells (L6) showed the same trends as antimalarial activity with **2** (1.1 μg/mL) being ~2-fold more potent than **3** (2.5 μg/mL), though the MIC values were at concentrations 50–100-fold higher than those needed for activity against *P. falciparum*. Interestingly, CDKs have been implicated as a promising target in *P. falciparum*[20] and kinase inhibitors have exhibited modest selective inhibition of ring stage parasites.[16] Thus, further elucidation of the relative contributions of the CDK 4 inhibitory, DNA intercalating, and hemozoin inhibitory activities to the remarkable selectivity of fascaplysin for ring stage over trophozoite and schizont stages holds promise for discovering effective treatments of malaria.

3. Experimental Section

3.1 General Experimental Procedures

Optical rotations were measured on a Jasco DIP-370 polarimeter. UV spectra were acquired in spectroscopy grade MeOH using a Hewlett-Packard 8452A diode array spectrophotometer. IR spectra were recorded on a JASCO FT/IR-420 spectrophotometer. NMR data of **1** were collected using a Varian INOVA 500 (^{1}H 500 MHz, ^{13}C 125 MHz) NMR spectrometer with a 3 mm Nalorac MDBG probe with a z-axis gradient and utilized residual solvent signals for referencing (δ_H 3.30, δ_C 49.00 for methanol-d_4). NMR data for **2** and **3** were obtained using a Varian Mercury 400 (^{1}H 400 MHz, ^{13}C 100 MHz) instrument equipped with a 5 mm Nalorac probe and utilized residual solvent signals for referencing as for compound **1**. High-resolution mass spectra (HRMS) were obtained using a Micromass Q-ToF micro. Analytical and semipreparative HPLC were accomplished utilizing a Beckman System Gold 126 solvent module equipped with a 168 PDA detector. All reagents were purchased and used without additional purification.

3.2 Biological Material

The *Didemnum* sp. ascidian was collected by SCUBA from Pratt Reef, Fiji Islands.[6]

3.3 Extraction and Isolation

This study started with material partially purified during the isolation of bengacarboline and fascaplysin.[6] A red fraction obtained from prior LH-20 column chromatography was subjected to HPLC on a Phenomenex Luna C18 column (250×10 mm) employing a gradient of 80:20 to 50:50 H_2O-MeCN (0.1% TFA) at 4 mL/min over 20 min to yield compound **1** (2.0 mg, t_R= 18.7 min), **2** (8.0 mg, t_R= 15.0 min), and **3** (11.0 mg, t_R= 13.4 min).

3.3.1 3-Bromohomofascaplysin A (1)—amorphous pale yellow-brown solid; $[\alpha]^{20}_D$ −9 (*c* 0.1, MeOH); UV (MeOH) λ_{max} (log ε) 404 (3.36), 336 (3.75), 270 (3.85), 232 (3.80), 212 (3.90) nm; IR (film) ν_{max} 3102, 2928, 2853, 1714, 1651, 1623, 1521, 1471, 1434, 1336, 1205, 1068, 1029, 952, 841, 802, 779, 751, 724, 645, 622,597,518 cm^{-1}; ^1H and ^{13}C NMR Table 1; HRESIMS *m/z* 409.0358 $[M+H]^+$ (calcd for $C_{21}H_{16}N_2O_2{}^{81}Br$, 409.0375; Δ −4 ppm).

3.4 Computational Chemistry

All calculations were performed using the Gaussian03 program. The potential energy surface of compound **2** in the gas phase was scanned at the AM1 level by rotating about the C-14-C-13 and C-15-C-14 bonds. Six conformers were located, of which three were relocated by full optimization at the B3LYP/6-31G** level in the gas phase. The geometries of the ground states were then used to calculate the ECD spectra by using TDDFT at the B3LYP/6-31G** level in the gas phase and at the B3LYP-SCRF/6-31G**//B3LYP/6-31G** level in MeOH with the COSMO model. The calculated excitation energies ΔE_i (in nm) and rotatory strength (R_i) were used to compute simulated ECD curves by using the Gaussian function:

$$\Delta \varepsilon(E) = \frac{1}{2.297 \times 10^{-39}} \frac{1}{\sqrt{2\pi}\sigma} \sum_i^A \Delta E_i R_i e^{-[(E-\Delta E_i)/2\sigma)]^2}$$

where σ is the width of the band at height $1/e$ and *i* represents an index over all transitions. In the current work, a value of $\sigma = 0.25$ eV and rotatory strength in the dipole length form (R_{len}) were used. The detailed calculation data are shown in the Supporting Information.

3.5 Detection of Life Stage-Specific Inhibition of *Plasmodium falciparum*

The flow cytometric analysis of malaria parasite growth was carried out as previously described.[16] In brief, asynchronous cultures of the chloroquine- and mefloquine-resistant *P. falciparum* strainW2-Mef (MRA-615 deposited to ATCC/MR4 by A. F. Cowman) were maintained at a 5% hematocrit in RPMI-1640 based malaria culture media. To determine the IC_{50} value, parasites were exposed to test drugs which were diluted in ½ log_{10} steps from 10 μM down to 0.33 nM. Cultures were then grown in triplicate for 48 hr. Cells were then stained with Hoechst 33342 (DNA), thiazole orange (RNA), $DiIC_1$-5 (membrane potential of live cells), and propidium iodide (membrane integrity) for 40 min. The combination of the DNA and RNA levels allowed for the determination of parasite erythrocytic life cycle stages (rings, trophozoites, or schizonts).[21] Calculation of IC_{50} values were carried out as described previously[16] by comparing the averaged number of parasites found in each concentration of drug across replicates and divided by the average number of corresponding parasites in control wells grown in the absence of any drug. To calculate IC_{50} values, a non-

linear sigmoid dose-response curve for variable slope was fitted to the data using GraphPad Prism version 5.00 for Windows (San Diego, CA).

Supplementary Material

Refer to Web version on PubMed Central for supplementary material.

Acknowledgments

References and Notes

1. Roll DM, Ireland CM, Lu HS, Clardy J. J Org Chem. 1988; 53:3276–3278.

2. Soni R, Muller L, Furet P, Schoepfer J, Stephan C, Zunstein-Mecher S, Fretz H, Chaudhuri B. Biochem Biophys Res Commum. 2000; 275:877–884.

3. Hörmann A, Chaudhuri B, Fretz H. Bioorg Med Chem. 2001; 9:917–921. [PubMed: 11354674]

4. Kinder FR, Bair KW, Bontempo J, Crews P, Czutchta AM, Nemzek R, Thale Z, Vattay A, Versace RW, Weltchek S, Wood A, Zabludoff SD, Phillips PE. Proc Am Assoc Cancer Res. 2000; 41:600–601.

5. Lin J, Yan XJ, Chen HM. Cancer Chemother Pharmacol. 2007; 59:439–445. [PubMed: 16816972]

6. Foderaro TA, Barrows LR, Lassota P, Ireland CM. J Org Chem. 1997; 62:6064–6065.

7. Jimènez C, Quiñoà E, Adamczeski M, Hunter LM, Crews P. J Org Chem. 1991; 56:3403–3410.

8. Kirsch G, König GM, Wright AD, Kaminsky R. J Nat Prod. 2000; 63:825–829. [PubMed: 10869210]

9. (a) Ireland C, Scheuer PJ. J Am Chem Soc. 1980; 102:5688–5691.(b) Roy RS, Gehring AM, Milne JC, Belshaw PJ, Walsh CT. Nat Prod Rep. 1999; 16:249–263. [PubMed: 10331285]

10. Molinski TF. Chem Rev. 1993; 93:1825–1838.

11. Schumacher RW, Davidson BS. Tetrahedron. 1995; 51:10125–10130.

12. Krishnaiah P, Reddy VLN, Venkataramana G, Ravinder K, Srinivasulu M, Raju TV, Ravikumar K, Chandrasekar D, Ramakrishna S, Venkateswarlu Y. J Nat Prod. 2004; 67:1168–1171. [PubMed: 15270574]

13. Vervoort HC, Pawlik JR, Fenical W. Mar Ecol Prog Ser. 1998; 164:221–228.

14. Davis RA, Sandoval IT, Concepcion GP, da Rocha RM, Ireland CM. Tetrahedron. 2003; 59:2855–2859.

15. Ding Y, Li XC, Ferreira D. J Org Chem. 2007; 72:9010–9017. [PubMed: 17958369]

16. Grimberg BT, Jaworska MM, Hough LB, Zimmerman PA, Phillips JG. Bioorg Med Chem Lett. 2009; 19:5452–5457. [PubMed: 19666223]

17. Wright CW, Addae-Kyereme J, Breen AG, Brown JE, Cox MF, Croft SL, Gökçek Y, Kendrick H, Phillips RM, Pollet PL. J Med Chem. 2001; 44:3187–3194. [PubMed: 11543688]

18. Bonjean K, De Pauw-Gillet MC, Defresne MP, Colson P, Houssier C, Dassonneville L, Bailly C, Greimers R, Wright C, Quetin-Leclercq J, Tits M, Angenot L. Biochemistry. 1998; 37:5136–5146. [PubMed: 9548744]

19. Onyeibor O, Croft SL, Dodson HI, Feiz-Haddad M, Kendrick H, Millington NJ, Parapini S, Phillips RM, Seville S, Shnyder SD, Taramelli D, Wright CW. J Med Chem. 2005; 48:2701–2709. [PubMed: 15801861]

20. Geyer JA, Prigge ST, Waters NC. Biochim Biophys Acta. 2005; 1754:160–170. [PubMed: 16185941]

21. Grimberg BT, Erickson JJ, Sramkoski RM, Jacobberger JW, Zimmerman PA. Cytometry A. 2008; 73:546–554. [PubMed: 18302186]
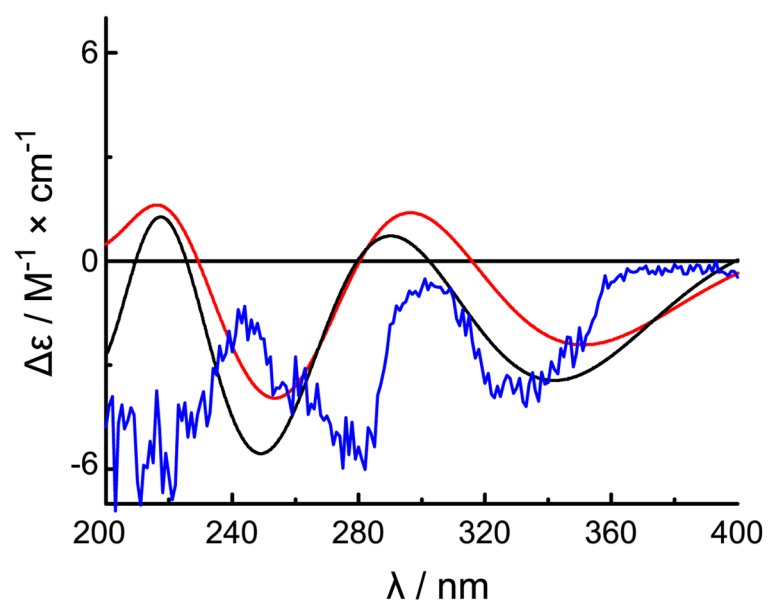
Figure 1.
Weighted ECD spectra of compound **2** in the gas phase at the B3LYP/6-31G** level (red) and in MeOH at the B3LYP-SCRF/6-31G**//B3LYP/6-31G** level with the COSMO Model in MeOH (black) and its experimental ECD spectrum in MeOH (blue).
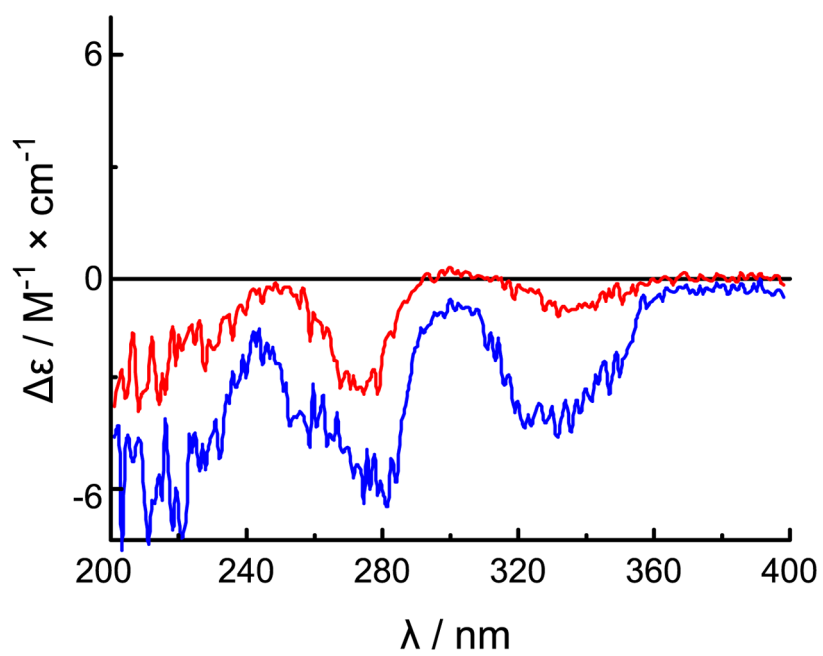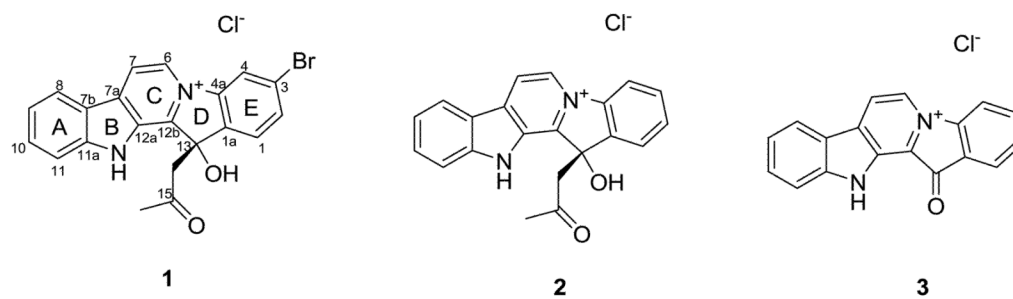
Figure 2.
The experimental CD spectra of compounds **1** (red) and **2** (blue) in MeOH.

Scheme.

Table 1

NMR data for compound **1** (^{1}H 500 MHz, ^{13}C 125 MHz, δ ppm) in methanol-d_4

position	δ$_C$	δ$_H$ mult. (*J* in Hz)	^{1}H-^{1}H COSY	HMBC
1	127.5 CH	7.80 m	H-2	C-3, C-4a, C-13
1a	138.0 C			
2	135.0 CH	7.82 m		C-1a, C-4
3	125.8 C			
4	119.2 CH	8.54 d (1.2)	H-2	C-4a, C-1a, C-2, C-3
4a	144.1 C			
6	125.3 CH	9.26 d (6.8)	H-7	C-12b, C-4a, C-7a, C-7
7	118.7 CH	8.77 d (6.8)		C-12a, C-7b, C-6, C-12b
7a	137.5 C			
7b	121.9 C			
8	124.8 CH	8.43 d (8.4)	H-9, H-10	C-11a, C-10, C-7b
9	124.0 CH	7.49 dd (8.4, 7.6)	H-10	C-10, C-7b, C-11
10	134.6 CH	7.83 m	H-11	C-11a, C-8, C-9
11	114.5 CH	7.82 m		C-11a, C-9
11a	147.5 C			
12a	132.4 C			
12b	145.0 C			
13	79.6 C			
14	51.6 CH$_2$	4.16 d (18.4)		C-15, C-12b, C-1a, C-13
15	206.7 C	4.26 d (18.4)		
16	30.4 CH$_3$	1.99 s		C-15, C-14, C-13

Table 2

Life stage-specific IC_{50} values[a] of **1**–**3** against *Plasmodium falciparum* strain W2-Mef

Cmpd.	All live parasites	Rings	Trophozoites	Schizonts
1	805 ± 50	574 ± 27	1189 ± 34	765 ± 81
2	105 ± 38	0.55 ± 0.11	252.18 ± 0.08	94 ± 90
3	48.2 ± 3.3	7.82 ± 0.13	401 ± 65	65.2 ± 9.8
chloroquine	149 ± 17	174 ± 32	162 ± 12	80 ± 2.8
artemisinin	6.245 ± 0.07	5.92 ± 0.17	6.46 ± 0.20	5.91 ± 0.27

[a]IC_{50} values given in nM.